



Pilot evaluation of a fracture process zone in a modified compact tension specimen by X-ray tomography

Jiří Klon, Stanislav Seitl, Hana Šimonová, Zbyněk Keršner

Brno University of Technology, Faculty of Civil Engineering, Veveří 331/95, 602 00 Brno, Czech Republic

klon.j@fce.vutbr.cz, <http://orcid.org/0000-0002-9551-2185>

seitl.s@fce.vutbr.cz, <http://orcid.org/0000-0002-4953-4324>

simonova.h@vutbr.cz, <http://orcid.org/0000-0003-1537-6388>

kersner.z@fce.vutbr.cz, <http://orcid.org/0000-0003-4724-6166>

Ivana Kumpová, Daniel Vavřík

Institute of Theoretical and Applied Mechanics AS CR, v. v. i., Prosecká 809/76, 190 00 Praha 9, Czech Republic

kumpova@itam.cas.cz, <http://orcid.org/0000-0001-8556-4996>

vavrik@itam.cas.cz, <http://orcid.org/0000-0002-8599-9903>

ABSTRACT. In the case of quasi-brittle material, there is a zone of non-linear behaving material, near the crack tip. A major part of this zone forms a so-called fracture process zone (FPZ), where mechanisms of material toughening take place. The main idea is to estimate the size of the fracture process zone under various types of load by using X-ray tomography. The estimation of the zone is supported by the theory of linear elastic fracture mechanics (LEFM) that could be a limit case of quasi-brittle mechanics. The size of the zone envelop is provided in X-ray snaps and compared with the theoretical size from LEFM.

KEYWORDS. Fracture process zone; X-ray; Concrete; Composites; Stress intensity factor; Compact tension specimen.



Citation: Klon, J., Seitl, S., Šimonová, H., Keršner, Z., Kumpová, I., Vavřík, D., Pilot evaluation of a fracture process zone in a modified compact tension specimen by X-ray tomography, *Frattura ed Integrità Strutturale*, 42 (2017) 161-169.

Received: 16.06.2017

Accepted: 21.07.2017

Published: 01.10.2017

Copyright: © 2017 This is an open access article under the terms of the CC-BY 4.0, which permits unrestricted use, distribution, and reproduction in any medium, provided the original author and source are credited.

INTRODUCTION

In the case of quasi-brittle materials, there is a zone of non-linear behaving material, near the crack tip. A major part of this zone forms a so-called *fracture process zone* (FPZ), where mechanisms of material toughening take place [1, 2]. Tensile softening is caused by these mechanisms. This softening is caused for example by crack deflection, crack bridging by the aggregate grain, friction of crack faces, blinding of cracks in the pores, crack branching, etc. The FPZ has recently begun to be considered in the models for description of quasi-brittle fracture. Mechanisms that take place in the FPZ and cause tensile softening in fact change mechanical parameters of the material [3]. The authors assume that one of the changed parameters is also material density, which is different for the main material, and the material that is in the FPZ.



In the FPZ it is not only the size and shape of the test specimen crucial for the development [4, 5], but also the boundary conditions of the test. For quasi-brittle materials (especially concrete, rocks, ceramics, etc.) we are talking about the so-called size effect, shape effect and boundary effect that affect the values of the fracture parameters [6, 7]. In order to detect or eliminate these influences, it is necessary to take into account the way that fracture spreads through quasi-brittle materials, in the so-called FPZ. The size and shape of this zone are related to the tension distribution in the specimen body, affected by the above mentioned boundary conditions and the specimen size and shape – degree of tension and deformation distress that changes near the crack tip.

This paper is focused on evaluation of the size and shape of the FPZ using X-ray imaging and computed tomography. This method is capable of capturing different material density values in individual parts of the whole volume of a tested specimen. This ability was used to determine the size and shape of the FPZ for two specimens made of quasi-brittle material. A fine-grained cement-based composite was selected as a suitable material. *Modified compact tension* (MCT) test specimens (The preparation of specimens and the MCT test are described below.) made of this material were used for determination of the size and shape of the FPZ. After the MCT test execution some parts close to the crack face were cut off from the specimens (see Fig. 1). These parts were used to perform X-ray imaging and computed tomography for evaluation of the size and shape of the FPZ.



Figure 1: Parts of MCT specimens cut off for X-ray tomography.

THEORETICAL BACKGROUND

X-ray tomography

The principle of X-ray imaging and computed tomography (CT) is generally well known in medical applications. X-rays penetrating the examined object are attenuated depending on the density, thickness and composition of the material according to the equation:

$$I = I_0 \cdot e^{-\mu d} \quad (1)$$

where I_0 is the initial intensity of the X-ray beam, I is the intensity of the X-ray beam after the penetration of the examined object, d is the thickness of the object and μ is the X-ray attenuation coefficient. Resulting intensity incidents individual pixels of the detector and its value is creating a grey scale image known as a radiogram or X-ray projection. During an X-ray CT, many of these projections are acquired at different angles. Modern CT systems use various shapes of an X-Ray beam (cone beam, fan beam, collimated beam), various acquisition geometries (conventional CT, helical CT, limited angle CT) as well as various methods of calculating the reconstruction of a 3D model (Filtered Back Projection - FBP, Ordered Subset Expectation Maximization – OSEM).

The visualization of the fracture process zone of the specimens presented in this paper was performed using conventional CT in the unique TORATOM (Twinned Orthogonal Adjustable Tomograph) device (Fig. 2), EP2835631. This advanced workstation combines two pairs of X-Ray tube-detectors in an orthogonal arrangement with fully motorized axes for geometry setting, which makes it possible to change the projection magnification from about 1.2 times to 100 times and the 3D volume resolution of 0.2 millimeters to units of micrometers. The orthogonal arrangement enables the Dual Source CT

(DSCT), which has two-fold acceleration of the process of collecting data for tomographic reconstruction, or Dual Energy CT (DECT), which allows to improve the visualization of differences between the material components with very similar or very different X-ray attenuation. System variability also provides a sufficient range for large area 2D scanning. Very stable high resolution is possible with regard to the installation of a high precision rotary stage and the use of an anti-vibration table, on which the whole assembly is placed. The details of X-ray measurement could be found in [8, 9].

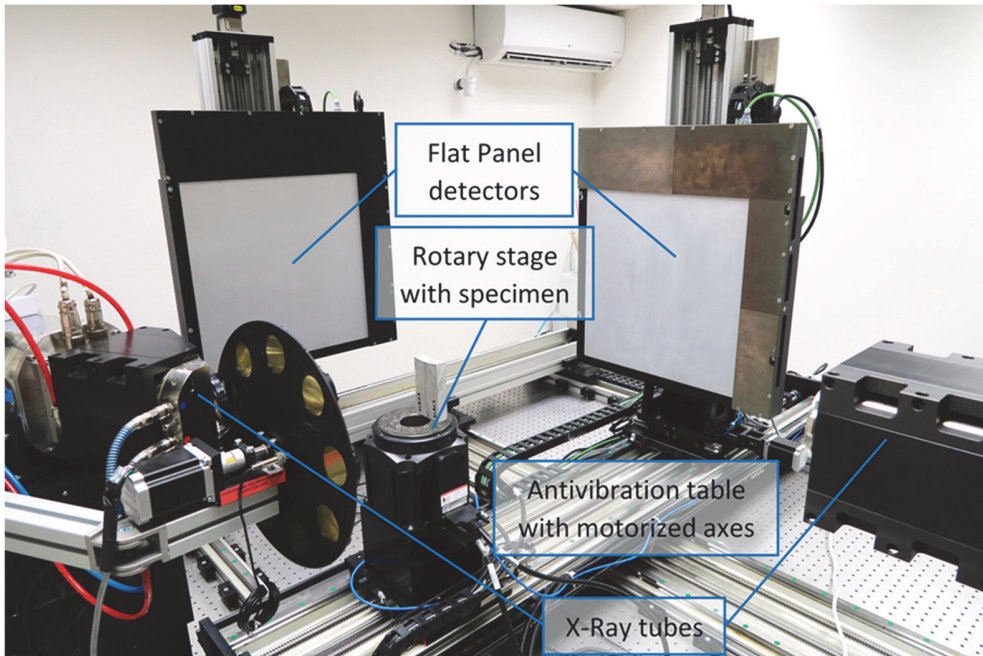


Figure 2: TORATOM (Twinned Orthogonal Adjustable Tomograph) in the Centre of Excellence Telč, Czech Republic.

MODIFIED COMPACT TENSION TEST

The *Modified compact tension* (MCT) test was used to capture changes of the shape and size of the FPZ. The modification of compact tension test configuration for its adaptation on quasi-brittle materials is based on changes of loading force eccentricity. This modification causes significant changes in stress distribution through the whole specimen body. A numerical study using the cohesive crack model of this test was shown in [10]. The contribution presents a parametric study focused on optimization of the introduction of the loading force eccentricity into the specimen for various configurations.

As the most suitable way of introducing the loading force, a variant with a rectangular shape of a specimen was selected. This specimen has a symmetrical stress concentrator in the shape of circular sectors on both shorter sides. In the narrow part of the specimen, between the circular sections, an initiation notch is performed. Loading is introduced by two steel platens glued on the specimen symmetrically on both longer sides. The thickness of the specimen and also the steel platens is 20 mm. Steel platens of two variants are used (1 and 2). The difference between the two variants of platens is in the eccentricity of introduced loading force. Loading force transmission from the test equipment to the specimen is realized through a loading head, which is connected to the platens with a pin. This pin allows free rotation of the specimen, so only pulling force is introduced (the specimen is not bent). By using these two platens, it is possible to make three test configurations:

- configuration A – eccentricity of loading force by 0.3 W' ,
- configuration B – eccentricity of loading force by 0.1 W' ,
- configuration C – eccentricity of loading force by -0.1 W' .

All configurations, except the dimensions are shown in Fig. 3. The characteristic dimension is W' , this is the specimen width at the narrowest point. This dimension is also the specimen height and the diameter of the above mentioned circular sectors (see Fig. 3).



Calibration curves for MCT

For a standard CT specimen it is defined as the polynomial function, see [11, 13], based on the following formula:

$$K_I = \frac{P}{B} \sqrt{\frac{\pi}{W}} F(a/W) \quad (2)$$

where K_I is the stress intensity factor for mode I, P is force, B is the thickness of the specimen, W is the width of the specimen and a is crack length. The calibration curves for the MCT specimen were published in [12] and their polynomial functions for the range $0.3 \leq a/W \leq 0.7$ are as follows:

$$F(\text{MCT A}) = 47.288 - 412.63\left(\frac{a}{W}\right) + 1403.5\left(\frac{a}{W}\right)^2 - 2039.7\left(\frac{a}{W}\right)^3 + 1127.4\left(\frac{a}{W}\right)^4 \quad (3)$$

$$F(\text{MCT B}) = 37.434 - 329.09\left(\frac{a}{W}\right) + 1119.2\left(\frac{a}{W}\right)^2 - 1626.5\left(\frac{a}{W}\right)^3 + 898.75\left(\frac{a}{W}\right)^4 \quad (4)$$

$$F(\text{MCT C}) = 27.729 - 246.48\left(\frac{a}{W}\right) + 837.45\left(\frac{a}{W}\right)^2 - 1216.7\left(\frac{a}{W}\right)^3 + 671.67\left(\frac{a}{W}\right)^4 \quad (5)$$

Initial estimation of the size of the fracture zone from a purely elastic solution (linear elastic fracture mechanics) under the condition of plane stress is as follows, see [13]:

$$r_y = \frac{1}{2\pi} \left(\frac{K_I}{\sigma_0} \right)^2 \quad (6)$$

where σ_0 is the material characteristic in tension.

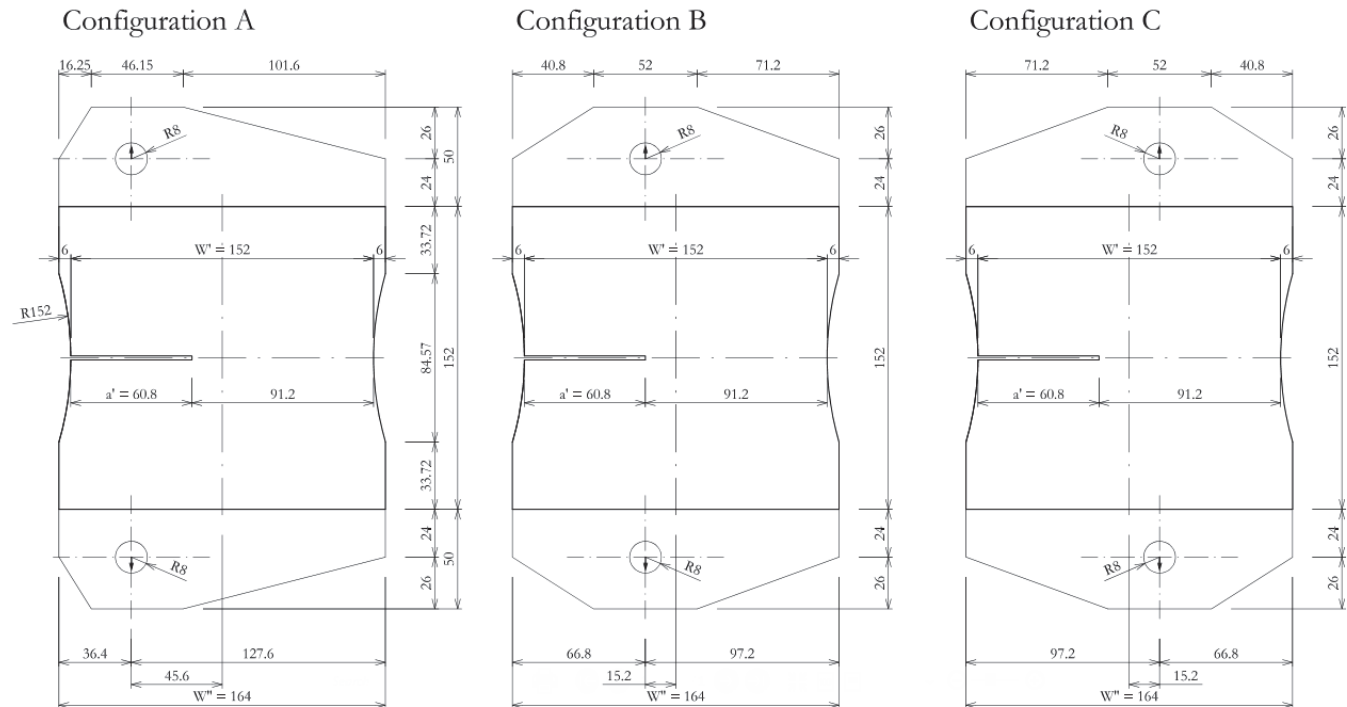


Figure 3: Scheme of test configurations of the MCT tests for specimens of size XL.

MATERIAL

Specimens were prepared from a fine grained cement-based composite, see [14]. A design of mixture composition is based on the standard ČSN EN 196-1 [15]. The fresh composite was made with quartzite sand with the maximum nominal grain size of 2 mm standardized according to ČSN EN 196-1 [15], Portland cement type 42.5 R and water in the ratio of 3:1:0.35 (S:C:W) with addition of a super-plasticizer SVC 4035 in the amount of 1 % by cement mass. This composite was chosen with respect to the previously verified appropriate response of the specimen for static loading (quasi-brittle fracture of the specimen). An idea of preparing the specimens can be formed from Fig. 4.

After one day of aging in constant relative humidity provided by foil coated molds, the test specimens were unmolded and stored in a water bath at laboratory temperature. After seven days, the specimens were removed from water, then exposed to free drying and an initiation notch was made with a diamond blade saw. After short drying steel platens were attached to the specimens using epoxy resins Sikadur-31 CF Rapid. The glue thickness was between 2–3 mm as recommended by the manufacturer. The test specimen and the method of sticking steel platens are shown in the pictures in Fig. 5.



Figure 4: Specimens preparation in silicone molds installed in frames made of waterproof plywood.

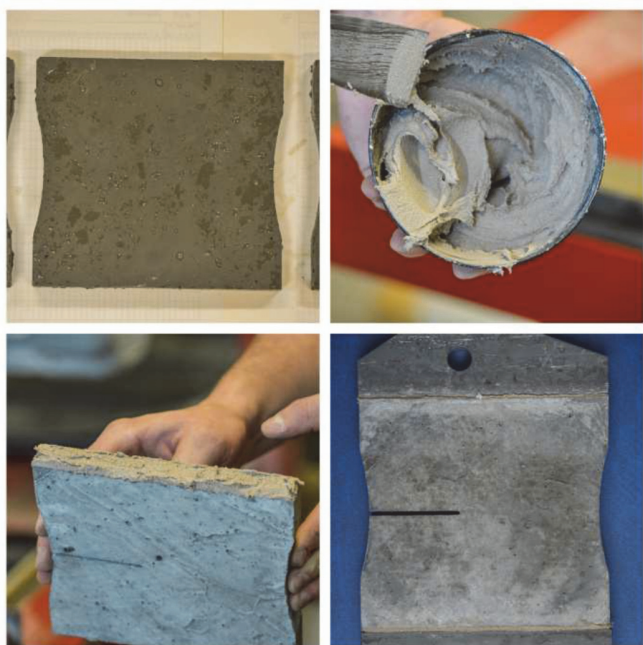


Figure 5: Specimen after its removal from the silicon mold and gluing of the steel platens to the notched specimen.

EXPERIMENTAL PROCEDURE

MCT fracture test

Pilot experiments of the MCT tests were performed on the LabTest 6.1000 testing machine (load range of 0 up to 1000 kN), which is located in the AdMaS Center, the Faculty of Civil Engineering, Brno University of Technology in Brno. The test was controlled by the prescribed displacement of the cross beam at a rate of 0.02 mm/min. Loading force P vs. crack mouth opening displacement ($CMOD$) was monitored and the prescribed cross beam deflection was verified. These values were monitored for all three test configurations (A, B and C). The set-up and detail of the fixture are shown in Fig.6.

X-ray tomography Measurement

XL-sized specimens broken during the MCT test with modified configurations A and B were cropped into the shape of an irregular block with the approximate dimensions of 105 × 20 × 30 mm. Samples were tomographically measured with one



pair X-Ray tube – detector. For CT scanning, a nanofocus X-Ray tube (XWT-240-SE, X-Ray WorX, Germany) operating in microfocus mode (spot size 4.0 μm) with a voltage of 220 kV, target current of 386 μA and power output of 85 W was used. Low energy photons, which do not contribute to the resulting image quality, were filtered using a 1.5 mm thick layer of brass. As a detector, a flat panel (XRD-1622-AP-14, Perkin Elmer, USA) with dimensions of 40 \times 40 cm, pixel matrix 2048 \times 2048 and 200 μm pixel size operating with a capacity of 0.5 pF was used. By geometry adjustment to the focus-detector distance of 1000.09 mm and focus-object distance of 326.23 mm, the projection magnification factor 3.07 was obtained, leading to the resolution of 65.24 μm per pixel in projections and 65.86 μm per voxel in 3D reconstructions. Geometrical parameters were chosen in order to obtain the best possible resolution with regard to the size of the samples and the detector area. For image correction in projection images, standard “dark field” and “open beam” correction, along with “beam hardening” correction (BHC), was used. Data for BHC were taken for a set of brass filters with thicknesses of 0, 0.3, 0.6, 0.9, 1.5, 3.0 and 6.0 mm, the correction image for each filter was averaged out of fifty images with the acquisition time of 1000 ms. For tomography, 1 200 projections were acquired, each with the exposure time of 1000 ms.



Figure 6: Overall view of the test machine with the specimen and selected details of the experiment.

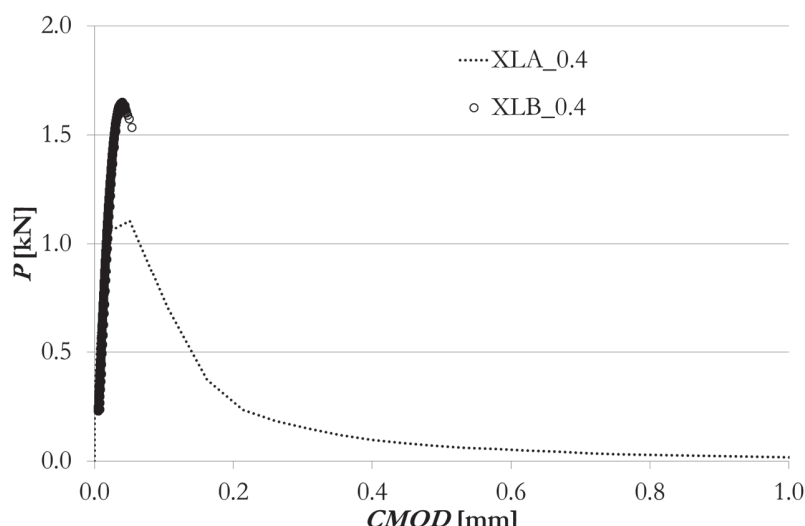


Figure 7: P -CMOD diagram of MCT A and MCT B tests.

For this reason only two samples were able to proceed X-ray tomography (configurations A and B). Because the entire specimen is not able to be scanned due to the resolution required (see section X-ray tomography), parts near the crack face from both sides were cut out of the specimen. The sizes of these parts were approximately $105 \times 20 \times 30$ mm. Because of time reasons, X-ray tomography was performed for only one part of each specimen.

RESULTS AND DISCUSSION

The MCT tests were successful for A and B variants, where the crack initiates from the initiation notch and leads through the specimen to the circle section on the opposite side. Required quasi-brittle fracture was achieved (for configuration B soon after the maximum loading force was reached, the specimen broke down, see P -CMOD diagram in Fig. 7). For variant C the test was unsuccessful, because the steel platens broke away from the specimen (no crack initiation from the initiation notch) see Fig. 6. This breach was caused due to bad adherence of the glue to the specimen. The specimen of variant C broke down by the initiate crack in the layer of glue and separated the specimen from the platen (see Fig. 6). This failure was probably caused by the high moisture of the specimen, when gluing the platens. Details from the performed tests are shown in Fig. 6.

Based on the informative value of average compressive cube strength from [16, 9] ($f_c = 55.1$ MPa), the value of tensile strength was determined according to the following formula [17]:

$$f_{ctm} = 0.3(f_{ck})^{2/3} \quad (7)$$

From Eq. (7), the value of tensile strength of material is $f_{ctm}=4.34$ MPa. Tab. 1 summarized details about the specimen dimension, relative lengths of the initial crack/notch, experimentally obtain the values of the maximal load and evaluated the values of fracture toughness and the size of the zone according to the LEFM theory (eq (6)).

Specimen	B [mm]	W [mm]	a/W [-]	P_{\max} [kN]	K_{Ic} [MPam $^{1/2}$]	r_y [mm]
MCT A	20	152	0.4	1.1049	1.285	0.0139
MCT B	20	152	0.4	1.6480	1.416	0.0169

Table 1: The dimension of the MCT specimen, the maximal value of force, fracture toughness and the size of the zone according to the LEFM theory.

The FPZ determined by using X-ray tomography on specimens of variants A and B are shown in Fig. 8 (variant A) and Fig. 9 (variant B). The determined FPZ is highlighted in blue. As can be seen from those two pictures, the FPZs for both variants are different. The difference between these two FPZs is caused by the above mentioned degree of tension and deformation distress that change near the crack tip. The FPZ for variant B is wider and its cumulative area is bigger than for variant A. This behaviour corresponds to the results of the numerical simulation performed with ATENA software [18]. Because the difference between these two FPZs is not too large, for future work it is necessary to use suitable advanced software to evaluate these differences.

CONCLUSIONS

It was proven that reduction of the material density in the course of the fracture process zone is detectable using X-ray tomography. For better quality results, smaller regions of interest should be chosen to improve the resulting resolution respectively. At the given magnification, microcracks cannot be detected properly and only a kind of nebula is visible in areas, where microcracking is expected.

The pilot X-ray tomography obtained results will be numerically verified by using an advanced software tool, see e.g. [19-21].

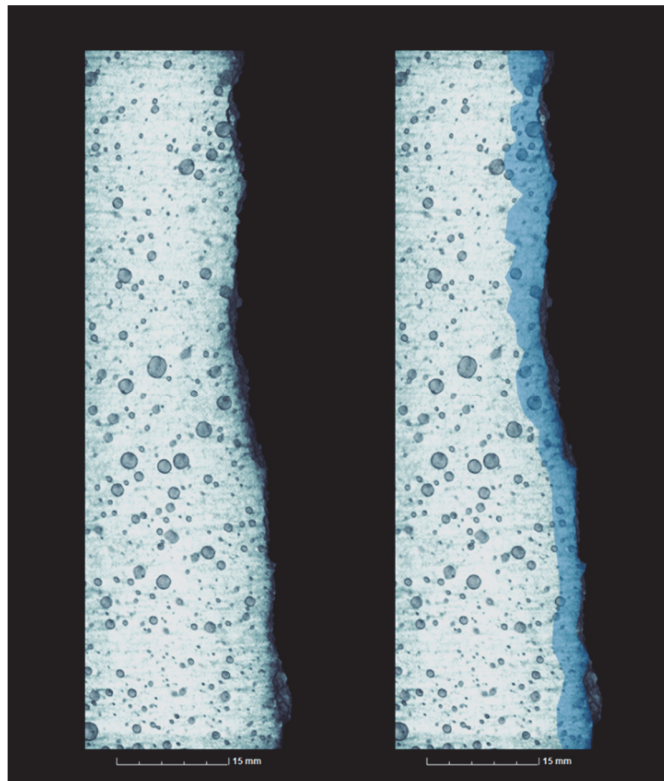


Figure 8: Visualization of the Specimen XLA_0.4 inner structure – area of microcracks propagation highlighted.

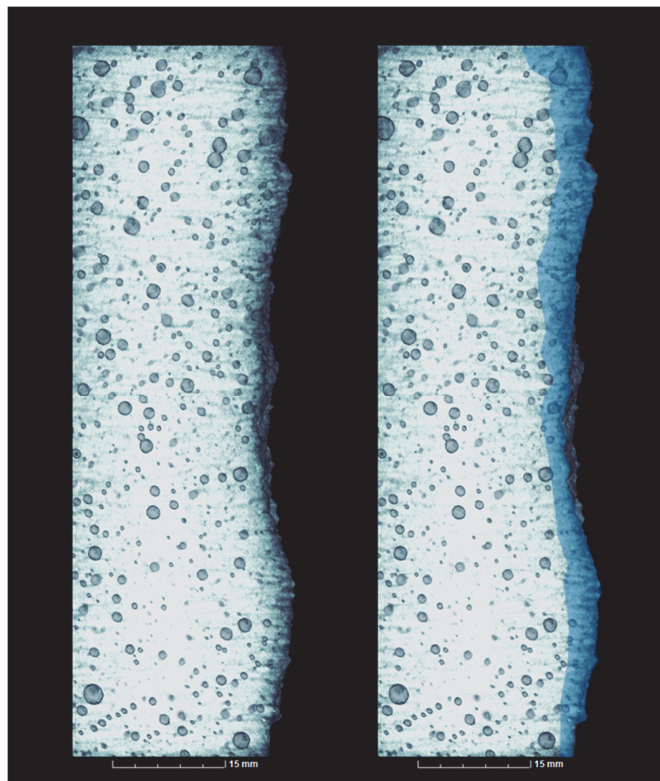


Figure 9: Visualization of the Specimen XLB_0.4 inner structure – area of microcracks propagation highlighted.

ACKNOWLEDGMENT

Financial support from the Czech Science Foundation: project 15-07210S. This paper has been worked out under the “National Sustainability Programme I” project “AdMaS UP – Advanced Materials, Structures and Technologies” (No. LO1408) supported by the Ministry of Education, Youth and Sports of the Czech Republic and Brno University of Technology, Specific Research programme (FAST-J-17-4638).

REFERENCES

- [1] Karihaloo, B.L., Fracture Mechanics and Structural concrete, New York: Longman Scientific & Technical, (1995).
- [2] Veselý, V., The role of process zone in quasi-brittle fracture, Habilitation thesis, BUT Brno, (2015).
- [3] Veselý, V., Keršner, Z., Merta, I., Quasi-brittle Behaviour of Composites as a Key to Generalized Understanding of Material Structure, Procedia Engineering, 190 (2017) 126–133. DOI: 10.1016/j.proeng.2017.05.317.
- [4] Korte, S., Boel, V., De Corte, W., De Schutter, G., Seitl, S., Experimental study of the influence of the initial notch length in cubical concrete wedge-splitting test specimens, Key Engineering Materials, 525–526 (2013) 209–212.
- [5] Seitl, S., Klusák, J., Keršner, Z., The influence of a notch width on a crack growth for various configurations of three-point bending specimens, Materials Engineering, XIV/3 (2007) 213–219.
- [6] Bažant, Z.P., Analysis of work-of-fracture method for measuring fracture energy of concrete, ASCE Journal of Engineering Mechanics, 122(2) (1996) 138–144.
- [7] Duan, K., Hu, X.-Z., Wittmann, F.H., Size effect on specific fracture energy of concrete, Engineering Fracture Mechanics, 74 (2007) 87–96.
- [8] Vavřík, D., Janděsek, I., Fíla, T., Veselý, V., Radiographic observation and semi-analytical reconstruction of fracture process zone in silicate composite specimen, Acta Technica, 58 (2013) 315–326.



- [9] Kumpová, I., Fíla, T., Vavřík, D., Keršner, Z., X-ray dynamic observation of the evolution of the fracture process zone in a quasi-brittle specimen, *J. Inst.*, 10 (2015). DOI: 10.1088/1748-0221/10/08/C08004.
- [10] Veselý, V., Sobek, J., Numerical study of failure of cementitious composite specimens in modified compact tension fracture test. *Transactions of the VŠB – Technical University of Ostrava*, 13(2) (2013), Civil Engineering Series, paper #25. DOI: 10.2478/tvsb-2013-0025.
- [11] Tada, H., Paris, P.C., Irwin, G. R., *The stress analysis of Cracks*, New York (2000) 677.
- [12] Seitl, S., Ríos, J.D., Cifuentes, H., Veselý, V., Effect of the load eccentricity on fracture behavior of cementitious materials subjected to the modified compact tension test, *Solid State Phenomena*, 258 (2017) 518–521. DOI: 10.4028/www.scientific.net/SSP.258.518.
- [13] Anderson, T. L., *Fracture mechanics fundamentals and applications*, CRC Press (1991).
- [14] Kucharczyková, B., Šimonová, H., Keršner, Z., Daněk, P., Kocáb, D., Misák, P., Pössl, P., Evaluation of Shrinkage, Mass Changes and Fracture Properties of Fine-aggregate Cement-based Composites during Ageing. *Procedia Engineering*, 109 (2017) 357–364. DOI: 10.1016/j.proeng.2017.05.349.
- [15] ČSN EN 196-1:2005, Methods of testing cement - Part 1: Determination of strength, Prague: ČNI, 2005, (the Czech version of the European Standard EN 196-1 (2005)).
- [16] Kucharczyková, B., Šimonová, H., Misák, P., Keršner, Z., Development of shrinkage and fracture parameters in selected fine-grained cement-based composites. In: Melcer, J., Kotrasová, K., eds. *MATEC Web of Conferences: Dynamics of Civil Engineering and Transport Structures and Wind Engineering – DYN-WIND'2017*. EDP Sciences – Web of Conferences, 107 (2017) 1–7. DOI: 10.1051/matecconf/201710700036.
- [17] ČSN EN 206 Concrete - Specification, performance, production and conformity (the Czech version of the European Standard EN 206).
- [18] Klon, J., Sobek, J., Keršner, Z., Modelling of modified compact tension test of fine-grained cement based concrete specimens using FEM software, *Key Engineering Materials*, in press (2018).
- [19] Klon, J., Veselý, V., Modelling of size and shape of damage zone in quasi-brittle notched specimens – analytical approach based on fracture-mechanical evaluation of loading curves, *Frattura ed Integrità Strutturale*, 39 (2017) 17–28. DOI: 10.3221/IGF-ESIS.39.03.
- [20] Veselý, V., Frantík, P., Reconstruction of fracture process zone during tensile failure of quasi-brittle materials, *Appl. Comp. Mech.*, 4(2) (2010) 237–250.
- [21] Veselý, V., Frantík, P., An application for the fracture characterisation of quasi-brittle materials taking into account fracture process zone influence, *Adv. Eng. Softw.*, 72 (2014) 66–76. DOI: 10.1016/j.advengsoft.2013.06.004.